

RESEARCH ARTICLE

The auto-inhibitory domain and ATP-independent microtubule-binding region of Kinesin heavy chain are major functional domains for transport in the *Drosophila* germline

Lucy S. Williams¹, Sujoy Ganguly^{2,*}, Philippe Loiseau^{1,‡}, Bing Fu Ng¹ and Isabel M. Palacios^{1,§}**ABSTRACT**

The major motor Kinesin-1 provides a key pathway for cell polarization through intracellular transport. Little is known about how Kinesin works in complex cellular surroundings. Several cargos associate with Kinesin via Kinesin light chain (KLC). However, KLC is not required for all Kinesin transport. A putative cargo-binding domain was identified in the C-terminal tail of fungal Kinesin heavy chain (KHC). The tail is conserved in animal KHCs and might therefore represent an alternative KLC-independent cargo-interacting region. By comprehensive functional analysis of the tail during *Drosophila* oogenesis we have gained an understanding of how KHC achieves specificity in its transport and how it is regulated. This is, to our knowledge, the first *in vivo* structural/functional analysis of the tail in animal Kinesins. We show that the tail is essential for all functions of KHC except Dynein transport, which is KLC dependent. These tail-dependent KHC activities can be functionally separated from one another by further characterizing domains within the tail. In particular, our data show the following. First, KHC is temporally regulated during oogenesis. Second, the IAK domain has an essential role distinct from its auto-inhibitory function. Third, lack of auto-inhibition in itself is not necessarily detrimental to KHC function. Finally, the ATP-independent microtubule-binding motif is required for cargo localization. These results stress that two unexpected highly conserved domains, namely the auto-inhibitory IAK and the auxiliary microtubule-binding motifs, are crucial for transport by Kinesin-1 and that, although not all cargos are conserved, their transport involves the most conserved domains of animal KHCs.

KEY WORDS: Cell asymmetries, Body plan, Oogenesis, Intracellular transport, Cytoskeleton, Microtubules, Motor proteins

INTRODUCTION

The transport of cargos by motors contributes to cytoplasmic heterogeneity. The motor protein Kinesin-1 (hereafter Kinesin) is responsible for the transport of cargos in most cell types and plays a crucial role in germline and neuronal polarization. Mutations in

the *Drosophila melanogaster* force-generating subunit of Kinesin, Kinesin heavy chain (KHC) result in defects in axonal transport (Hirokawa et al., 2010), localization of developmental determinants (Gagnon and Mowry, 2011) and movement of lipid droplets (Welte, 2009). A mouse model has also implicated Kinesin in axonal process growth (Karle et al., 2012).

Biochemical investigations have elucidated important aspects of the walking mechanism of KHC (Gennerich and Vale, 2009), but how Kinesin discriminates among its cargos and which domains are involved in cargo interaction are not yet understood. Several cargos associate with Kinesin via Kinesin light chain (KLC), a major partner of KHC. KLC binds to coil-3 of the KHC stalk [amino acids (aa) 771–813 and 792–836 of human and *Drosophila* KHC; Fig. 1A] (Diefenbach et al., 1998; Loiseau et al., 2010) and mediates interaction of the motor with various cargos, including JNK-interacting protein (JIP) vesicles (Bowman et al., 2000; Gauger and Goldstein, 1993; Gindhart et al., 1998; Verhey et al., 2001) and the KASH proteins involved in nuclear migration (Meyerzon et al., 2009). However, KLC is not required for the association of all cargos with Kinesin. For example, in neurons the localization of mitochondria and FMRP (FMR1) occurs in a KLC-independent manner (Glater et al., 2006; Ling et al., 2004). In the case of *Drosophila* mitochondria, KHC binds Milton, which in turn binds Miro, a mitochondrial GTPase. Milton competes with KLC for its binding to KHC (Glater et al., 2006). In addition, some cargo adaptors seem to bind both KLC and KHC, as shown for DISC1 (Taya et al., 2007) and Sunday driver (Syd; *Drosophila* JIP) (Sun et al., 2011).

The mechanisms that target Kinesin to specific cargos outside of the neuron are less well understood. For example, in the *Drosophila* oocyte, neither KLC nor the KLC-like protein Pat1 [which is redundant with KLC (Loiseau et al., 2010)] plays a major role in the KHC-dependent localization of the developmental determinant *oskar* mRNA, in KHC-dependent positioning of the nucleus or in the induction of cytoplasmic streaming (Brendza et al., 2002; Duncan and Warrior, 2002; Januschke et al., 2002; Loiseau et al., 2010; Palacios and St Johnston, 2002). Studies on *Neurospora crassa* (which lacks KLCs) have identified a putative cargo-binding domain in the C-terminus of KHC, which is conserved in animal KHCs (aa 850–950, Fig. 1A, Fig. 5A) (Seiler et al., 2000). Furthermore, brain microsomes and GRIP1 bind to this region in sea urchin and mouse KHC, respectively (Setou et al., 2002; Skoufias et al., 1994; Yu et al., 1992). This region, which is known as the tail, might therefore represent an alternative cargo-binding domain that could account for some of the KLC-independent functions of KHC. In addition to the *N. crassa* putative cargo-binding domain, the tail has two other conserved regions, which comprise the auto-inhibitory IAK motif (Coy et al., 1999; Friedman and Vale, 1999; Stock et al., 1999) and an auxiliary ATP-independent microtubule (MT)-binding site (Hackney and Stock,

¹University of Cambridge, Zoology Department, Downing Street, Cambridge CB2 3EJ, UK. ²University of Cambridge, DAMTP, Wilberforce Road, Cambridge CB3 0WA, UK.

*Present address: Molecular Cell Biology and Genetics Max Planck Institute, Plotenhauerstrasse 108, Dresden, 01307 Germany. [‡]Present address: Genewave SAS, 172 Rue de Charonne, 75011 Paris, France.

§Author for correspondence (mip22@cam.ac.uk)

This is an Open Access article distributed under the terms of the Creative Commons Attribution License (<http://creativecommons.org/licenses/by/3.0>), which permits unrestricted use, distribution and reproduction in any medium provided that the original work is properly attributed.

2000; Jolly et al., 2010; Navone et al., 1992; Seeger and Rice, 2010; Yonekura et al., 2006) (Fig. 1A, Fig. 5A).

To provide details of the functional structure of the C-terminal region of KHC, as well as to gain further insight into how KHC carries out its various transport functions, we performed a structural/functional analysis of the motor (excluding the motor domains) in the *Drosophila* oocyte. The germline is a unique model system in that it permits the study of Kinesin in a living cell in which several cargos are known and easily detectable, and the assessment of the developmental impact of modifying Kinesin function. This is achieved by analyzing Kinesin function in oocytes that lack endogenous KHC and only express mutated versions of the motor (tagged to GFP). Studying eggs that arise from these mutant oocytes assesses the developmental impact of the mutated motor. To our knowledge, this is the first structural/functional study on animal KHC, adding data to the study performed in fungi (Seiler et al., 2000).

RESULTS

The tail of KHC is essential for localization of *oskar* mRNA but not for Dynein transport

The two most conserved regions at the C-terminal end of animal KHCs are the KLC-binding domain (aa 792-839 and 771-818 in *Drosophila* and human KHCs, respectively) and the tail domain (aa 850-975 and 829-929 in *Drosophila* and human KHCs, respectively). We first investigated cargo localization using a KHC

that lacks the tail but contains the KLC-binding site (KHC1-849GFP, Fig. 1A) (Loiseau et al., 2010). A full-length motor (KHC1-975GFP) rescues all of the *Khc*²⁷ null mutant phenotypes in the oocyte (Fig. 1B,C, Fig. 2E, Table 1, Fig. 6B; supplementary material Figs S1, S3). However, *oskar* mRNA (detected by Staufen antibodies) is never localized to the posterior pole in *Khc* mutant oocytes (*Khc*²⁷ germline clones, GLCs) that express KHC1-849GFP ($n=80$, Fig. 1D), indicating that amino acids 850-975 are required for *oskar* transport. KHC1-849GFP has a similar expression level to, and dimerizes with, endogenous KHC (Loiseau et al., 2010) (supplementary material Fig. S2), and localizes to the posterior, with and without endogenous motor (Fig. 1D,E; data not shown).

In contrast to its inability to rescue *oskar* mRNA transport, KHC1-849 does rescue the transport of Dynein, which is found at the posterior in all KHC1-849 oocytes ($n=10$, Fig. 1E). Note that although Dynein is transported from the anterior to the posterior by KHC1-849, its posterior localization is not completely wild type. Since *oskar* mRNA, but not Dynein, requires the KHC tail for its transport to the posterior, this suggests that KHC has domain-specific functions in the germline.

Although KLC is not essential for KHC function in *Drosophila* oocytes (Loiseau et al., 2010; Palacios and St Johnston, 2002), it is unknown whether the KLC-binding site itself is required for the establishment of asymmetry. Oocytes expressing a truncated motor lacking the last 275 amino acids (KHC1-700GFP) have a Dynein localization phenotype indistinguishable from that of *Khc* null

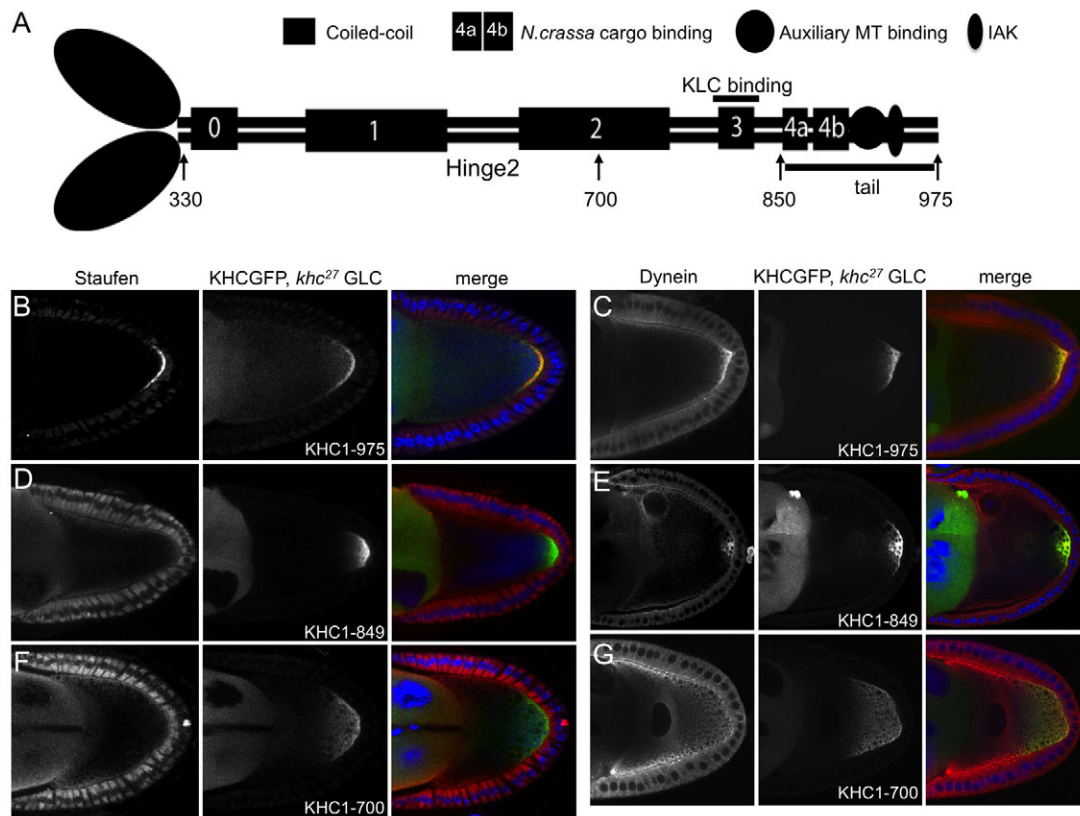


Fig. 1. KHC has cargo-specific domains. (A) *Drosophila* KHC consists of a motor domain followed by a series of coiled-coils (represented by boxes 0-4b). KLC binds to coil3. The tail contains three conserved domains: the auto-inhibitory IAK domain, the ATP-independent MT-binding site, and the *N. crassa* putative cargo-binding domain, which is within coils 4a/b. (B-G) Immunohistochemistry for Staufen or Dynein (red in merge) in st9 *Khc*²⁷ oocytes (germline clones, GLCs) containing KHC-GFP transgenes (green in merge). (B,C) A full-length KHC (KHC1-975) rescues the posterior localization of Staufen (B) and Dynein (C). (D,E) KHC lacking the last 126 amino acids (KHC1-849) cannot transport Staufen (D) but can still transport Dynein (E). (F,G) KHC lacking the last 275 amino acids (KHC1-700) cannot transport Staufen (F) or Dynein (G). DAPI, blue. The anterior of the oocyte is to the left in this and subsequent figures unless stated otherwise.

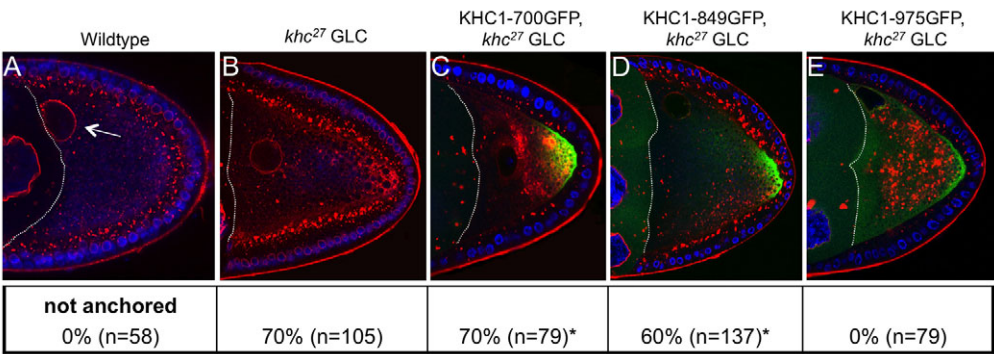


Fig. 2. Two domains of KHC act to position the nucleus. Membranes are stained with fluorescent wheat germ agglutinin (red) in st9 wild-type (A) and *Khc²⁷* oocytes (GLCs) without (B) or with KHC-GFP transgenes (green in C-E). White line indicates the anterior membrane. (A) Wild-type nucleus positioning to the anterior-dorsal corner (arrow, note that the nucleus is in contact with the anterior membrane, but that the view axis is partially rotated). (B) In *Khc* null oocytes the nucleus is no longer attached to the anterior cortex. (C) An equivalent phenotype is observed in KHC1-700 oocytes. (D) Tailless KHC1-849 is able to weakly rescue nucleus positioning. (E) Full-length KHC fully rescues nucleus positioning. DAPI, blue. **P*=0.088 (left) and **P*=0.95 (right) for KHC1-700 versus KHC1-849 (Fisher's exact test), considered to be not statistically significant.

oocytes (*n*=12, Fig. 1G) (Duncan and Warrior, 2002; Januschke et al., 2002; Palacios and St Johnston, 2002). This result, together with the posterior localization of Dynein in KHC1-849 oocytes, suggests that amino acids 701-849 (containing the KLC-binding site) are required for Dynein transport. KHC1-700GFP has a similar expression level to that of the endogenous motor and localizes to the posterior, with and without endogenous motor (Fig. 1F,G; supplementary material Fig. S2; data not shown).

The phenotypes observed in both KHC1-849GFP and KHC1-700GFP egg chambers demonstrate that KHC-mediated cargo transport is domain specific and not via a common mechanism.

Both the tail and 701-849 region are required for positioning of the oocyte nucleus and establishment of the embryonic DV axis

Nucleus positioning is required for a number of cellular and developmental events. The importance of this process is exemplified by the link between abnormal nucleus localization in muscle cells and myopathies. In *Drosophila*, the localization of the oocyte nucleus to the anterior-dorsal corner (Fig. 2A; supplementary material Fig. S1) is an early step in the establishment of the embryonic dorsal-ventral (DV) axis, since the dorsal determinant Gurken localizes around the nucleus and signals to the overlying follicle cells to take up a dorsal fate (supplementary material Fig. S1A). As a consequence, dorsal cells differentiate into two dorsal appendages (DAs) on the egg. When nucleus positioning or Gurken signaling is affected, the appendages are malformed or missing (Neuman-Silberberg and Schüpbach, 1993).

In 70% (*n*=105) of oocytes without KHC, the nucleus is not properly positioned and is found separated from the anterior

membrane by more than half a nucleus radius (Fig. 2B, distance defined arbitrarily as a nucleus positioning defect). This is also the case in KHC1-700 oocytes (*n*=79, Fig. 2C). Oocytes expressing the tailless KHC1-849 show a mild improvement in nucleus placement, with nuclei aberrantly positioned in 60% of the mutant oocytes (*n*=107, Fig. 2D). The full-length KHC1-975 fully rescues the localization of the nucleus in *Khc* mutants (*n*=79, Fig. 2E). To study the developmental impact of the mislocalization of the nucleus, we analyzed DA formation in KHC1-700 and KHC1-849 eggs. As with the nucleus, full-length KHC completely rescued the formation of the DAs (supplementary material Fig. S1), whereas 67% and 52% of the KHC1-700 and KHC1-849 eggs, respectively, have no DA (Table 1). Therefore, both the KHC tail and the region 701-849 are required for Kinesin to position the nucleus and to establish the DV axis.

Although there are more KHC1-849 eggs than KHC1-700 eggs with DAs, removing the tail blocks the formation of completely normal appendages, since only 3.5% of the KHC1-849 eggs have two fully formed DAs (Table 1). This suggests that Gurken signaling is strongly affected in KHC1-700, partially rescued by KHC1-849, but not fully rescued by any of these transgenes. This is confirmed by the observation that KHC1-849 oocytes are defective for Gurken localization, even when the nucleus seems properly positioned (supplementary material Fig. S1). This differential effect of KHC on the nucleus and on Gurken is also observed in *Khc* null oocytes (Brendza et al., 2002). Only 14% of stage (st) 9 KHC1-849 oocytes have normal Gurken protein distribution, and in most oocytes Gurken is either not closely associated with the nucleus or shows diffuse expression. This is a stronger defect than the nucleus positioning phenotype, suggesting that the DA defect of the tailless KHC is due to KHC1-849 having defective localization of both Gurken and nucleus.

These results indicate that both the tail and the KLC-binding regions are involved in proper nucleus and Gurken localization by KHC, and thus in establishing the embryonic DV axis.

The nucleus positioning function of KHC requires its motor activity

Motors might act as static anchors of cargos (Delanoue and Davis, 2005; Delanoue et al., 2007). Since oocytes with slow KHC show no defects in nucleus positioning, we investigated whether Kinesin requires its motor activity in order to ‘anchor’ the nucleus. We

Table 1. The DA phenotypes of wild-type and *Khc* mutant eggs

Genotype (n)	Normal (%)	Fused/one (%)	None (%)
Wild type (284)	97.5	1.4	1.1
<i>Khc²⁷</i> GLC; KHC1-975/+ (79)	96.2	3.8	0
<i>Khc²⁷</i> GLC; KHC1-849/+ (401)	3.5	44.4	52.1
<i>Khc²⁷</i> GLC; KHC1-700/+ (212)	3.3	29.2	67.5
<i>Khc²⁷</i> GLC (401)	0.7	17.0	82.3

KHC1-849 and KHC1-700 eggs both have strong DA defects, but there are statistically significant differences between these two mutant KHCs regarding the absence of DAs or the presence of one/fused DA [*P*<0.0001 (one-tailed)].

studied nucleus positioning in *Khc*²⁷ oocytes expressing KHC330-975GFP, a KHC that lacks the motor domain (Fig. 1A). This motorless Kinesin, in contrast to the posterior localization of wild-type KHC (Fig. 1B; supplementary material Fig. S3E,F), accumulates at the anterior/lateral cortex, where the minus ends of MTs are thought to be prevalent (supplementary material Fig. S3B,G,H) (Cha et al., 2002; Parton et al., 2011). Both nucleus positioning and DA formation are abnormal in KHC330-975 oocytes (supplementary material Fig. S3B,D), demonstrating that the motorless KHC is unable to sustain these processes. A motor that lacks the ATP-binding domain (KHC231-975) behaves equivalently to KHC330-975 (data not shown). KHC330-975 also phenocopies the *Khc* null mislocalization phenotype of Staufen and Dynein (supplementary material Fig. S3G,H). Although it is unknown how direct the action of KHC is on the positioning of the nucleus, it is interesting to note that KHC330-975GFP localizes to the oocyte nuclear membrane. This is also observed with full-length KHC, although with an additional punctate localization not seen with motorless KHC (supplementary material Fig. S3B,C).

More than one KHC dimer is present on posterior cargos

In the presence of endogenous Kinesin, KHC231-975 and KHC330-975 localize to the posterior (Fig. 3A; data not shown). This raises the question of how these motorless Kinesins reach this pole, as they cannot transport themselves there in the absence of KHC (Fig. 3B; supplementary material Fig. S3). Either they interact with cargos moved by wild-type Kinesin, or they form heterodimers with endogenous KHC and move by an unexpected ‘inchworm’ mechanism. To distinguish these hypotheses, we expressed both KHC231-975 and KHC1-604betaGal in a *Khc* null background. KHC1-604betaGal is a truncated form of KHC that moves on MTs and localizes to the posterior, but is without all known cargo-binding domains. If these two mutant Kinesins were able to heterodimerize and move (the inchworm model), both motors would be detected at the posterior. If, however, they cannot move together, then the

motorless KHC should remain at the anterior whereas KHC1-604betaGal would appear at the posterior. Only KHC1-604betaGal was found at the posterior (Fig. 3, 100%, *n*=15), suggesting that the posterior localization of KHC231-975 requires a cargo moved by another KHC molecule. Therefore, we can conclude that motorless KHC, and by extrapolation KHC, can be moved to the posterior by binding to cargos moved by other active motors, and that more than one KHC dimer can bind to a cargo being moved to the posterior. This correlates with previous work on lipid droplet transport (Shubeita et al., 2008). Whether ‘hitchhiking’ is relevant to KHC activity remains to be seen.

Developmental differences in Kinesin function

The behavior of KHC tail truncations highlights that Kinesin has distinct mechanisms of action within the same cell. For example, the tail is important for *oskar* RNA localization and nucleus positioning but does not affect Dynein transport. To fully characterize Kinesin function, we studied another process that is dependent on KHC: streaming of the ooplasm. From mid-oogenesis, there is constant mixing of the ooplasm driven by KHC-dependent transport (Ganguly et al., 2012; Palacios and St Johnston, 2002; Serbus et al., 2005). At st9, the movement is slow (Table 2). At st11, the flows are faster and more organized (Fig. 4; supplementary material Movie 1) (Dahlgard et al., 2007; Ganguly et al., 2012; Theurkauf, 1994). It is unknown to what extent streaming is relevant for cargo transport, but flows aid *nanos* RNA transport (Forrest and Gavis, 2003) and may help *oskar* localization (Ganguly et al., 2012).

In *Khc* mutants, streaming is completely absent at both mid- and late oogenesis. Both the early/slow and late/fast streaming are rescued by KHC1-975 (data not shown). When analyzing the streaming speed of KHC1-849 oocytes we observed a complex temporal phenotype whereby KHC1-849 cannot uphold streaming at st9 but by st11 streaming is of wild-type speed and appearance (Fig. 4, Table 2; supplementary material Movie 2). We observed a transition at st10B in KHC1-849 oocytes, in which there are regions

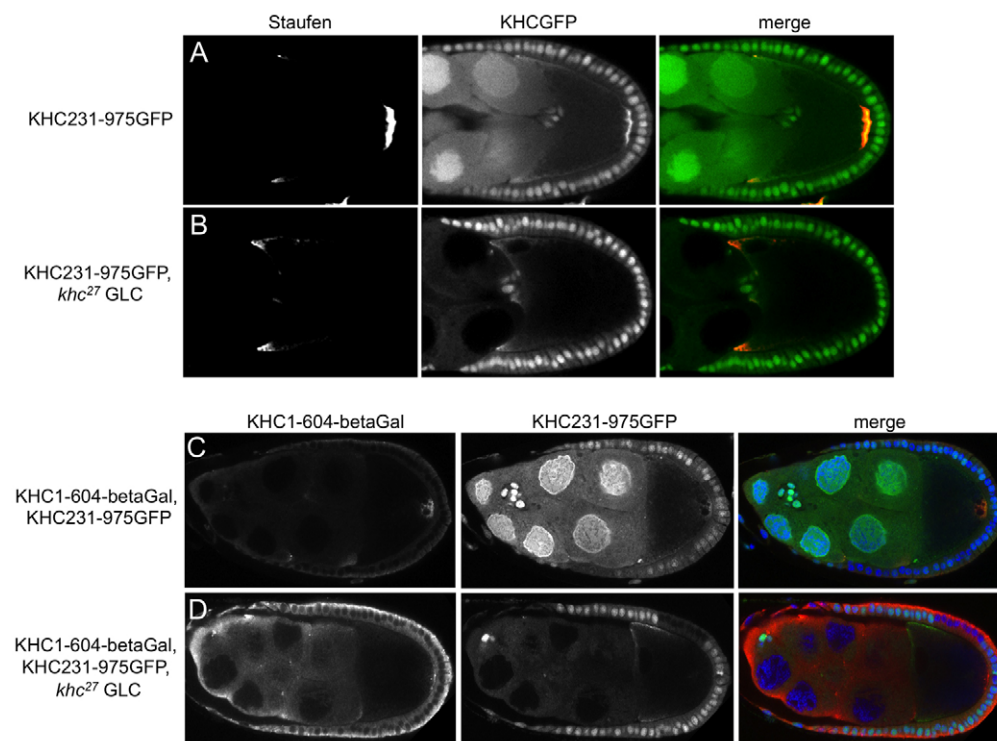


Fig. 3. More than one KHC dimer binds to posterior cargos.

(A,B) Staufen (red in merge) in KHC231-975GFP (green in merge) oocytes, in the presence (A) or absence (B, *Khc*²⁷ GLC) of endogenous KHC. KHC231-975 is transported to the posterior only in the presence of endogenous KHC. (C,D) Localization of KHC1-604betaGal (red in merge) and KHC231-975GFP (green in merge) in the presence (C) or absence (D) of endogenous KHC. DAPI, blue. The presence of nuclear GFP is a consequence of the mutant clone selection protocol and is not related to KHC-GFP. *Khc* mutant cells lack nuclear GFP (e.g. germline in B and D).

Table 2. Streaming speeds in wild-type and mutant stage 9 and 11 oocytes

Genotype	st9	st11
Wild type	21.5±0.8 nm/s (n=21)	109±7.6 nm/s (n=9)
KHC1-849, <i>Khc</i> ²⁷ GLC	—	111.7±7 nm/s (n=6)
KHC1-604, <i>Khc</i> ²⁷ GLC	—	—
<i>Khc</i> ²⁷ GLC	—	—
KHC330-975, <i>Khc</i> ²⁷ GLC	—	—

—, No discernible flows.

of fast flows in the center of the oocyte, surrounded by regions where streaming is not observed (data not shown). This transition might correlate with the actin cytoskeleton re-organization that occurs at st10B, when a cytoplasmic actin mesh is seen to disintegrate, initiating from the center of the oocyte (Dahlgaard et al., 2007). Our findings show that removing the tail has a different impact on flows depending on the developmental stage, allowing cytoplasmic streaming at st11 but not at st9.

Novel *in vivo* role for the auto-inhibitory IAK domain

The tail is dispensable for Dynein transport or late streaming, but it is essential for *oskar* transport, DV axis and st9 streaming. The tail contains three conserved motifs: the auto-inhibitory IAK motif, the auxiliary ATP-independent MT-binding site (hereafter, AMB), and the *N. crassa* putative cargo-binding domain (Fig. 5A). To characterize the function of these domains in *oskar* transport, we deleted the last 65 amino acids of KHC, creating KHC1-910GFP, which lacks the IAK and the AMB domains, but still contains the *N. crassa*-like domain. Although KHC1-910 localizes efficiently to the posterior (Fig. 5B), and is expressed at similar levels to endogenous KHC (supplementary material Fig. S4), *oskar* ribonucleoprotein (RNP) is mainly found at the anterior/lateral cortex of KHC1-910 oocytes, similar to in *Khc* null oocytes (Fig. 5B, n=35). Upon close inspection of the phenotype, however, it seems that a small amount of Staufen reaches the posterior. This would suggest that KHC1-910 activity in *oskar* RNA transport is severely constrained.

To further investigate which of the two conserved domains removed in KHC1-910 (i.e. IAK or AMB) is responsible for *oskar* transport, we obtained oocytes that only express a KHC in which the sequence QIAKPIR has been mutated to alanines (KHC1-975ΔIAK) (Ganguly et al., 2012) and thus lacks the auto-inhibitory domain (Fig. 5A; supplementary material Fig. S4). In these KHC1-

975ΔIAK oocytes, Staufen is found at the posterior and not at the anterior/lateral cortex as in KHC1-910 oocytes. Thus, the IAK domain is not essential for *oskar* transport.

Although KHC1-975ΔIAK oocytes accumulate Staufen at the posterior, this localization is not completely wild type, since Staufen is found in a ‘cloud’ next to a tight posterior crescent (Fig. 5C, 97%, n=34). Since this motor has no auto-inhibitory domain, it is possible that this cloud phenotype is due to the motor being excessively active. However, a dominant effect of KHC1-975ΔIAK on Staufen is made worse by removing a copy of endogenous KHC (supplementary material Fig. S4D), which might suggest that removing the IAK makes KHC less active in RNA transport. This result is also in agreement with the fact that a point mutation from QIAKPIRS to QIAKSIRS or from QIAKPIRS to QIAKPIRF results in inhibition, rather than overactivation, of some Kinesin-mediated transport (Moua et al., 2011).

We then analyzed how other KHC-dependent processes are affected when the IAK motif is removed. Interestingly, and in contrast to the weak defects observed for *oskar* localization, KHC1-975ΔIAK oocytes show a strong nucleus positioning phenotype (Table 3A, 30%). Accordingly, DA formation is also affected in KHC1-975ΔIAK eggs (Table 3B, 9% normal DAs). A striking *Khc* mutant phenotype is the presence of actin spheres close to the mislocalized nucleus (Januschke et al., 2002; Mische et al., 2007). This is a strongly penetrant *Khc* null phenotype, affecting 91% of *Khc* oocytes (Fig. 6). To fully describe the IAK function we looked more carefully at the formation of these aberrant actin spheres. Although never seen in wild-type or KHC1-975 oocytes (Fig. 6B; data not shown), these spheres are present in 84% of KHC1-975ΔIAK (Fig. 6C) and in 74% of KHC1-849 (Fig. 6D) oocytes. These spheres contain Rabenosyn-5 [a Rab5 effector protein (Tanaka and Nakamura, 2008)] (supplementary material Fig. S5), suggesting that vesicle trafficking is affected in *Khc* mutant oocytes. Interestingly, these ectopic vesicles seem to nucleate actin, as suggested when filming their behavior in the presence of Utrophin-GFP (supplementary material Fig. S5).

In vitro studies have shown that the IAK can interact with the motor domain to hinder ADP release and reduce processive movement. To distinguish whether the phenotypes observed in the KHC1-975ΔIAK oocytes are due to a lack of auto-inhibition or to the loss of function of the KHC1-975ΔIAK motor, we analyzed Staufen and DAs when amino acids 521-641 (Hinge2, Fig. 1A) are deleted (Barlan et al., 2013). The KHC auto-inhibited conformation is achieved by the motor folding in half at Hinge2, and deletion of

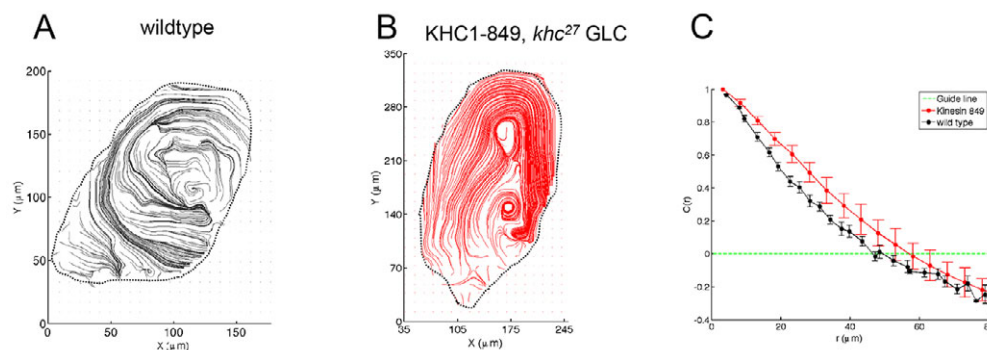


Fig. 4. Streaming phenotypes are developmentally regulated. Cytoplasmic streaming shows a stage-specific requirement for amino acids 849-975 (see also Table 2). (A,B) Streamline picture of one time point of wild-type (A, black) and KHC1-849 (B, red) st11 streaming. The cell is outlined (dotted line). (C) Correlation length distribution for wild-type versus KHC1-849 st11 streaming. The correlation length is a statistical measure of the radii of the flow features (Ganguly et al., 2012). The guide line (green) aids visualization of the correlation length. Bars indicate s.e. A *t*-test ($P=0.70$) and a Kolmogorov–Smirnov test ($P=0.53$) indicate that the correlation lengths in wild-type and KHC1-849 late stages are statistically identical.

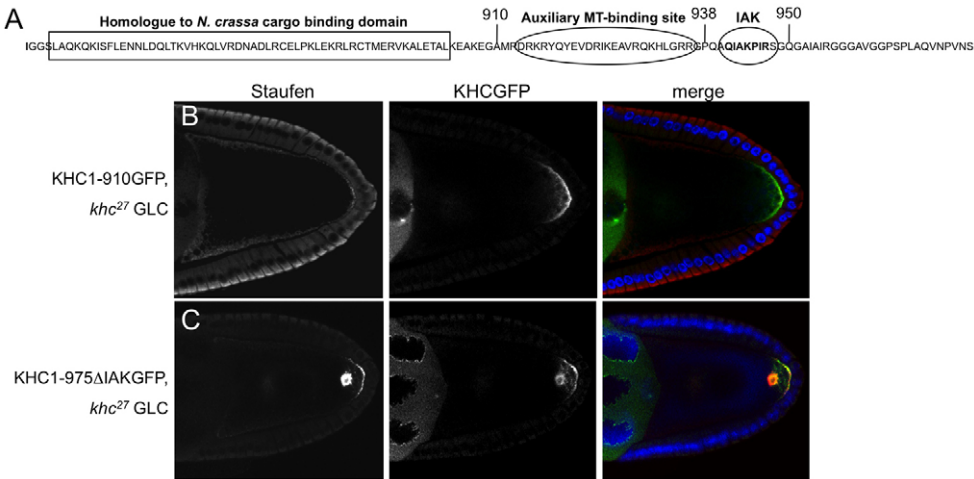


Fig. 5. Multiple specific functions of the tail. (A) The amino acid sequence of the KHC tail showing the three conserved domains. (B,C) Staufen (red in merge) and KHC-GFP transgene (green in merge) in st9 *Khc*²⁷ mutants (GLCs) containing KHC1-910GFP (B) and KHC1-975ΔIAKGFP (C). DAPI, blue.

this ‘flexible’ sequence is sufficient to disrupt tail-mediated repression of Kinesin (Friedman and Vale, 1999). KHC1-975ΔHinge2 oocytes show weak *oskar* localization defects (Fig. 7A, *n*=43) and no aberrant actin spheres (*n*=24). Furthermore, most KHC1-975ΔHinge2 eggs have normal DAs (Table 4). It is thought that auto-inhibition might prevent the mislocalization of Kinesin and futile ATP depletion. Our data suggest that KHC auto-inhibition does not play a major role in the oocyte.

Together, these results show that the IAK has functions other than auto-inhibition. This motif is required for KHC to be fully functional, and it is important for cargos such as the nucleus and actin spheres/vesicles and for the establishment of the DV axis. However, it is dispensable for st9 streaming (Ganguly et al., 2012) and the transport of *oskar* mRNA. *oskar* localization is a function of Kinesin that is not rescued by KHC1-910, a truncated motor with the *N. crassa*-like domain but that lacks the AMB region. Therefore, we next investigated whether the AMB site affects RNA transport.

An ATP-independent MT-binding domain at the C-terminus is essential for *oskar* RNA transport

The deletion of the last 37 amino acids creates a motor (KHC1-938GFP) that contains all conserved domains within the tail (including the AMB site) except the IAK and an uncharacterized motif (aa 955-959, IRGGG, which is conserved from *Drosophila* to mammals). Similarly to KHC1-975ΔIAK, 33% of the KHC1-938 oocytes show aberrant nucleus positioning (Table 3A) and DA formation is strongly affected in KHC1-938 eggs (Table 4, 16% normal DAs). Also, as with KHC1-975ΔIAK, oocytes expressing KHC1-938 show the aberrant accumulation of actin-recruiting spheres (supplementary material Fig. S6O). Most importantly, Staufen is mainly found at the posterior in KHC1-938 oocytes (Fig. 7B) and not at the anterior/lateral cortex as in KHC1-910 oocytes

(Fig. 5B). Specifically, the KHC1-938 oocytes show Staufen in a tight posterior crescent, but also in a posterior dot (Fig. 7B, 76% of oocytes with dots, *n*=25). This result shows that the addition of the AMB domain to KHC1-910 (resulting in KHC1-938) restores the capacity for KHC to transport *oskar* to the posterior. This suggests that the MT-binding site at the C-terminus of KHC (the AMB domain) is essential for *oskar* RNA transport, ascribing a novel function to this domain. Although *oskar* is not a conserved cargo, its transport involves one of the most conserved domains of animal KHCs (Kirchner et al., 1999b).

DISCUSSION

The oocyte allows the analysis of the C-terminal region of KHC in an *in vivo* context. Our results show that the interaction of Kinesin with its cargos and/or the regulation of the motor is complex and relies on more than one region. The tail (aa 850-975) is essential for all functions of KHC in the st9 oocyte except Dynein transport. These functions include the positioning of the nucleus and Gurken protein (and consequently establishment of the DV axis), the localization of *oskar*, the induction of streaming, and the distribution of actin-recruiting vesicles. Most of these tail-dependent KHC activities can be functionally separated from one another by further characterizing the conserved domains within the tail (supplementary material Fig. S7). The various functional domains are not necessarily involved in cargo binding, but their presence is required for wild-type cargo transport. In particular, our data show the following: (1) a temporal regulation of the impact of KHC activity on cytoplasmic streaming during oogenesis; (2) a novel essential role for the IAK that is distinct from its auto-inhibitory function; (3) that lack of auto-inhibition in itself is not necessarily detrimental to KHC function; and (4) that the AMB motif is required for *oskar* RNA localization.

Table 3. Nucleus positioning and DA phenotypes of KHC tail domain mutants

A. Nucleus positioning phenotypes				
<i>Khc</i> ²⁷ GLC plus:	KHC1-975	KHC1-975ΔIAK	KHC1-849	KHC1-938
Nucleus not anchored % (<i>n</i>)	0 (79)	30 (30)	60 (137)	33 (26)
B. DA phenotype of mutant eggs				
Genotype (<i>n</i>)	Normal (%)	Fused/one (%)	None (%)	
KHC1-975, <i>Khc</i> ²⁷ GLC (79)	96.2	3.8	0	
KHC1-975ΔIAK, <i>Khc</i> ²⁷ GLC (156)	9	36	55	
KHC1-849, <i>Khc</i> ²⁷ GLC (401)	3.5	44.4	52.1	

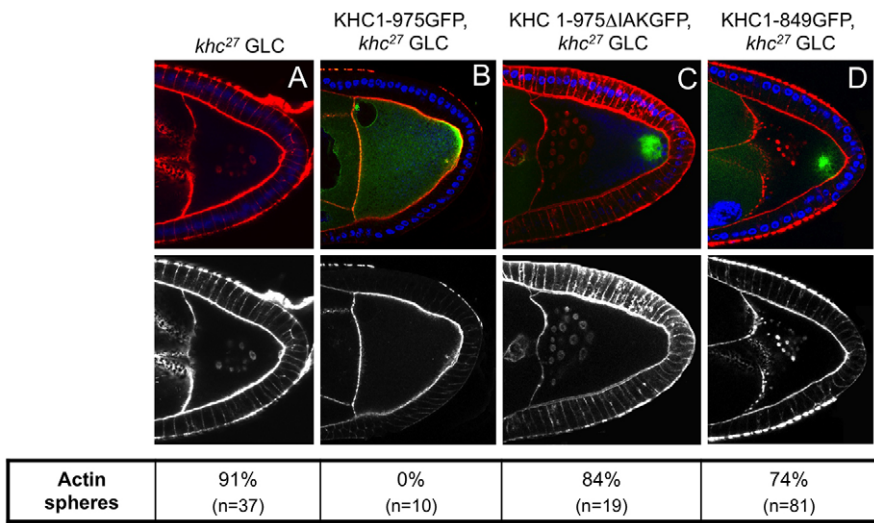


Fig. 6. Defective actin sphere formation in *Khc* null oocytes is due to the loss of the IAK motif. (A–D) F-actin (phalloidin, red in top row, white in bottom row) in st9 *Khc*²⁷ mutants (GLC) containing no transgene (A), or containing KHC1-975GFP (B), KHC1-975ΔIAKGFP (C) or KHC1-848GFP (D). DAPI, blue.

KLC and Pat1 are essential only for the KHC-dependent localization of Dynein

The localization of Dynein to the posterior requires Kinesin (Brendza et al., 2002; Duncan and Warrior, 2002; Januschke et al., 2002; Palacios and St Johnston, 2002). Here we show that deletion of the tail has a weak effect on the transport of Dynein, whereas further deletion of the region covering coil3 and half of coil2 renders a motor unable to localize Dynein. This observation correlates with the finding that KLC, which together with Pat1 mediates Dynein localization, interacts with coil3 of KHC in a tail-independent manner (Loiseau et al., 2010). It is then likely that Dynein is a posterior cargo of KHC, and that the Dynein complex interacts with KHC via KLCs. In *C. elegans*, the KLC-binding protein Jip3 binds Dynein light intermediate chain (Dlic) (Arimoto et al., 2011). However, *jip3/syd* mutant oocytes show no defects in the posterior localization of Dynein (Palacios and St Johnston, 2002). Alternatively, KLC might bind the Dynein intermediate chain (DIC), as in mammals (Ligon et al., 2004). This observation, together with the fact that amino acids 795–839 (including coil3) are conserved in animal KHCs, makes it plausible that, in the oocyte, KHC localizes Dynein via a coil3-dependent KLC-DIC complex.

It is important to keep in mind that even though KLC and the KLC-like protein Pat1 are not essential for the localization of *oskar* and the nucleus, or for the induction of flows, they still contribute to these KHC-dependent processes, albeit in a minor manner. *Pat1* mutants have slightly slower flows (Ganguly et al., 2012), and *Pat1,Klc* double mutants show mild *oskar* and nucleus localization defects in 78% and 9%, respectively, of the mutant oocytes (Loiseau et al., 2010) (data not shown). These nucleus anchoring defects might correlate with those seen in KHC1-700 oocytes, since KHC1-700 does not contain the KLC-binding domain; however, the nucleus phenotypes in KHC1-700 may not be statistically significantly different from those observed in KHC1-849 oocytes.

The tail domain of KHC is important for anterior-posterior and dorsal-ventral axes

oskar RNA is found at the anterior/lateral regions of the *Khc* mutant oocyte (Brendza et al., 2000). Similarly, *Khc*²⁷ st9 oocytes show a mispositioned nucleus and an aberrant distribution of Gurken protein (Brendza et al., 2002; Duncan and Warrior, 2002; Januschke et al., 2002). Consequently, embryos resulting from *Khc*²⁷ oocytes have an aberrant anterior-posterior (AP) and DV body plan. Deletion of the tail produces a motor that is unable to localize *oskar* RNA and thus

is unable to support the establishment of the AP axis. Further characterization of the function of conserved domains within the tail suggests that RNA transport activity relies on the AMB site.

In addition, 96.5% of the embryos resulting from tailless KHC oocytes have aberrant DA formation. This DV axis defect might be due to more than the tail function in nucleus positioning, since the nucleus is not positioned in 60% of tailless KHC1-849 oocytes. We show that KHC1-849 oocytes are defective for Gurken protein localization, even when the nucleus seems properly positioned. Given that the oocyte nucleus is associated with one of the MT-organizing centers (Januschke et al., 2006), it is possible that the defects in Gurken signaling, and thus DV axis, in Kinesin mutants are a result of both nucleus mispositioning and the misorganization of the anterior MTs (Brendza et al., 2002). This is consistent with MT defects observed at the anterior of KHC1-849 and KHC1-700 oocytes (supplementary material Fig. S6F,G,I, arrows). In wild-type and KHC1-975 oocytes, there is an obvious AP gradient of MTs, with a population of enriched MTs close to the anterior/lateral cortex (supplementary material Fig. S6A,B). This gradient can also be seen in some KHC1-849 and KHC1-700 oocytes (supplementary material Fig. S6E,H). However, most of these mutant oocytes show an extension of this anterior ‘bright’ MT network towards the posterior around the nucleus (supplementary material Fig. S6F,G), as well as the misorganization of MTs in a pattern that resembles the aberrant vesicles often detected at the anterior of *Khc* mutant oocytes (supplementary material Fig. S6F,I, arrows; vesicles in Fig. 6). The region encompassing the KLC-binding domain might also contribute to the establishment of the DV axis, since the number of oocytes with Gurken in an anterior-dorsal crescent drops from 14% in KHC1-849 oocytes to 0% in KHC1-700 oocytes (supplementary material Fig. S1).

Does KHC act directly on oocyte nucleus positioning and Gurken protein localization?

At first glance, it is unclear why there are nucleus and Gurken localization defects in the *Khc* null, when plus ends are biased towards the posterior (Parton et al., 2011). As nucleus positioning requires the Dynein complex, it follows that KHC function could be indirect for the anterior cargos, for example via the recycling of Dynein (Brendza et al., 2002; Duncan and Warrior, 2002; Januschke et al., 2002; Lei and Warrior, 2000; Swan et al., 1999; Swan and Suter, 1996; Zhao et al., 2012). However, we think that KHC could be acting directly on nucleus positioning. First, it cannot be

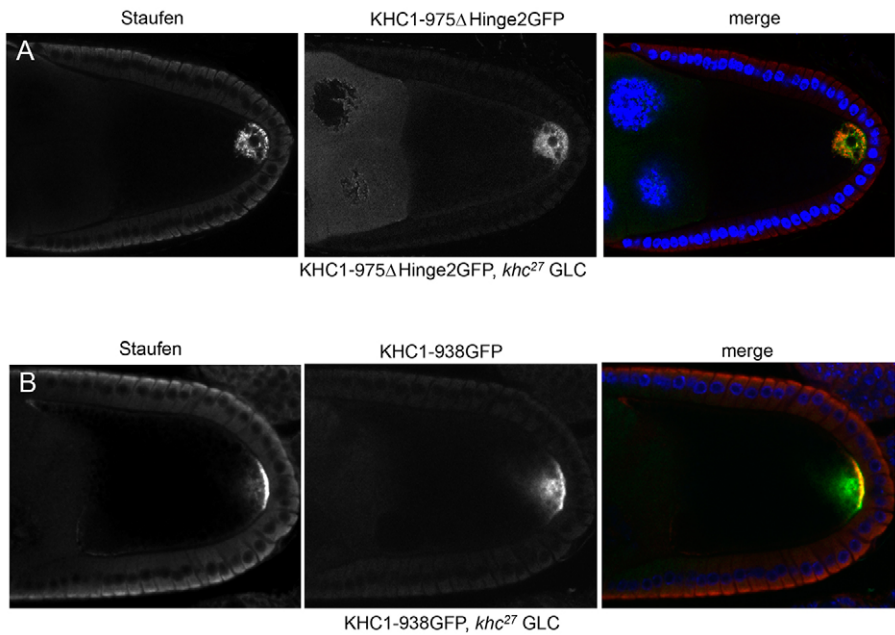


Fig. 7. Effect on cargo transport of deleting Hinge2 or the last 37 amino acids of KHC. (A) KHCΔHinge2 does not have equivalent phenotypes to KHCΔIAK (see also Table 4). Staufien (red in merge) in a st9 *Khc*²⁷ oocyte (GLC) containing KHC1-975ΔHinge2 (green in merge). (B) KHC1-938 is able to localize *oskar* mRNA to the posterior of the oocyte. Staufien (red in merge) in a st9 *Khc*²⁷ mutant oocyte (GLC) containing KHC1-938GFP (green in merge). DAPI, blue.

discounted that Dynein and Kinesin act independently: Dynein localization to the posterior is abolished in *Pat1*, *Klc* double mutants, whereas nucleus positioning is only weakly affected, suggesting that the coordinated action of the two motors is not necessarily required. Second, the MT network is complex, and there seem to be some plus ends towards the anterior cortex that Kinesin may harness (Parton et al., 2011). Third, KHC localizes at the nuclear envelope. Fourth, when KHC is missing, alpha-tubulin and Jupiter-GFP [a MT-associated protein fused to GFP (Ganguly et al., 2012; Karpova et al., 2006)] are found in dots at the nuclear envelope (data not shown) in a similar punctate pattern to that displayed by KHC.

All these preliminary observations might suggest that KHC is acting on a set of MTs that allows positioning of the nucleus in close proximity to the anterior membrane: when KHC is missing, these MTs seem to ‘collapse’ to the nuclear envelope and their stable existence is not maintained. Taking work on cultured cells (Splinter et al., 2010) into consideration, Kinesin might well bind to the nuclear envelope and transport the nucleus towards the plus ends. However, it is likely that the relative importance of different molecular links between the nuclear envelope and motors depends on the cell type (Splinter et al., 2010). For example, *Drosophila* SUN/KASH proteins (Msp-300, Klarsicht and Klaroid) have no essential functions during oogenesis (Technau and Roth, 2008). Mammalian KHC is also known to bind directly to the nucleoporin Ranbp2 via its tail (Splinter et al., 2010).

There are other mutants that show nucleus positioning defects, including *skittles* (which encodes phosphatidylinositol 4,5-bisphosphate-synthesizing enzyme) (Gervais et al., 2008), *trailer hitch* (*tral*) and *Bicaudal C* (*BicC*). Among these, *tral* and *BicC* mutants have abnormal actin-covered vesicles that look similar to those

present in *Khc* oocytes (Kugler et al., 2009; Snee and Macdonald, 2009). This similarity, together with our data showing that Rabenosyn-5 is present in *Khc* mutant vesicles, suggest that KHC is required for membrane trafficking in the oocyte. This correlates with the function of KHC in other cells and with the observation that, in *Khc* oocytes, Rab6 vesicles aggregate abnormally around the mispositioned nucleus (Januschke et al., 2007). The ectopic vesicles that we observe in *Khc* oocytes seem to nucleate actin, as seen in time-lapse movies of Utrophin-GFP. As suggested for *tral* and *BicC*, the formation of ‘actin spheres’ (as a readout of vesicle trafficking problems) in *Khc* oocytes might cause defects in Gurken signaling. In fact, Gurken is detected in close proximity to actin-recruiting vesicles in KHC1-938 oocytes (supplementary material Fig. S6O, arrow). These data stress that the anterior phenotypes observed in *Khc* mutant oocytes are likely to be the result of a complex relationship between vesicle trafficking, MTs and nucleus location. Ectopic sites of actin also appear in *Rab5* (Compagnon et al., 2009), *Rab6* (Januschke et al., 2007), *IKK-related kinase* (*IκB kinase-like 2* – FlyBase) (Shapiro and Anderson, 2006) and *spn-F* (Abdu et al., 2006) oocytes. They were interpreted as cytoskeleton defects, but might also be the result of ectopic actin nucleation by aberrantly distributed vesicles.

Novel in vivo functions for the IAK motif

Auto-inhibition to limit the consumption of ATP/GTP by motors not bound to cargos is conserved in Myosins (Jung et al., 2008; Li et al., 2006; Umeki et al., 2009) and Kinesins (Al-Bassam et al., 2003; Imanishi et al., 2006; Seiler et al., 2000). As both protein families share a common ancestor, it is not unexpected that there is a common mechanism to this auto-inhibition, in which the tail folds back to the motor domain. It is clear from research on affecting

Table 4. The DA phenotypes of wild-type and *Khc* mutant eggs

Genotype (n)	Normal (%)	Fused/one (%)	None (%)
Wild type (284)	97.5	1.4	1.1
KHC1-975ΔHinge2, <i>Khc</i> ²⁷ GLC (130)	77	18	5
KHC1-975ΔIAK, <i>Khc</i> ²⁷ GLC (156)	9	36	55
KHC1-938, <i>Khc</i> ²⁷ GLC (96)	16	30	54

KHC1-975ΔHinge2 and KHC1-975ΔIAK eggs do not have equivalent DA defects.

auto-inhibition *in vivo* that these motors cannot function correctly, leading to detrimental transport (Al-Bassam et al., 2003; Imanishi et al., 2006; Seiler et al., 2000). What was still unknown is whether the defects in transport are a consequence of a lack of inhibition or are due to alternative functions of the motifs involved. We have compared these two hypotheses directly for the first time.

Recently, the stoichiometry of the interaction between the IAK and motor domains has been determined, with one IAK motif per motor dimer required (Hackney et al., 2009). This has led to the suggestion that the other motif could be free to bind cargo or other regulators of KHC. A mutant IAK with two individual point mutations (IAK_{PIRS} to IAK_{SIRS}, IAK_{PIRS} to IAK_{PIRSE}) shows weak defects in *oskar* transport and DA formation that are similar to those of *Khc* hypomorphic alleles, suggesting that these mutations result in inhibition rather than overactivation of transport (Moua et al., 2011). Similarly, the IAK seems to facilitate, rather than downregulate, axonal transport of mitochondria. However, these IAK point mutants did not constitute a full null of IAK activity, since when we mutagenize the entire motif the DA defects are much stronger than those observed in the point mutants. In addition, deletion of the IAK phenocopies the deletion of the tail regarding the formation of dorsal structures, with only a slight increase in the number of normal DAs in IAK mutant oocytes (9% in IAK oocytes versus 3.5% in KHC1-849 oocytes, Table 3B).

A hypothesis to explain the cargo transport defects observed in KHC1-975ΔIAK oocytes, which are not observed in KHC1-975ΔHinge2 oocytes, is that KHC1-975ΔIAK has reduced function for these cargoes. That is to say, the IAK motif has an essential activity that is independent of its auto-inhibition function. Interestingly, the streaming speed of KHC1-975ΔIAK is faster than wild type (Ganguly et al., 2012), suggesting that KHC1-975ΔIAK is not defective for all KHC functions. Instead, the increased streaming speed might be due to the number of motors that are active at any one time being higher. This correlates with many more particles of KHC1-849 than of KHC1-975 moving in *in vitro* assays (Loiseau et al., 2010).

Our results with KHCΔHinge2 show that auto-inhibition does not play a major role in transport during oogenesis. However, there seems to be a small contribution of auto-inhibition to DA formation, in accordance with work on fungal kinesin showing that maintenance of the folded conformation partially contributes to growth rates (Kirchner et al., 1999a). In conclusion, KHC auto-inhibition might not be such an important driving factor as previously thought, especially not in the oocyte. It might be interesting to analyze how a lack of auto-inhibition affects KHC function in other cells, such as neurons.

Novel *in vivo* role for the auxiliary MT-binding site

The region 850-910 is conserved between all animal and fungal KHCs and contains the *N. crassa* putative cargo-binding domain. However, KHC1-910 does not support wild-type localization of *oskar* or wild-type streaming. It is however possible that KHC1-910 is able to bind cargo but is somehow unable to transport it. This could be the case for *oskar* RNA, since there is a weak accumulation of the transcript at the posterior in KHC1-910 oocytes. If KHC1-910 binds *oskar*, but its action is constrained, one would expect an enrichment of KHC1-910 at the anterior/lateral cortex, where *oskar* accumulates. We do not detect higher levels of KHC1-910 than of KHC1-975 in that region, and thus it is uncertain how small amounts of *oskar* reach the posterior in KHC1-910 oocytes.

The localization of wild-type amounts of *oskar* RNA to the posterior is rescued when the AMB site is restored in KHC1-938,

demonstrating a key role of this domain in cargo localization. This supports the observation that mutations in this region (four arginines) render a severe *Khc* allele with reduced motor function in neurons (Moua et al., 2011). This AMB region binds to MTs *in vitro* and in cells, perhaps via electrostatic interactions (Hackney and Stock, 2000; Jolly et al., 2010; Navone et al., 1992; Seeger and Rice, 2010; Yonekura et al., 2006), and seems responsible for an MT polymerization activity of the tail (Seeger and Rice, 2010). Furthermore, KHC slides and bundles MTs in cells (Jolly et al., 2010) and, in the case of fungal Kinesin, this MT bundling activity depends on the tail (Straube et al., 2006). How does this MT regulatory function of the domain relate to the capacity of KHC1-938 to localize *oskar*? The MTs of KHC1-938 and KHC1-910 oocytes still form an AP gradient, seemingly of wild-type topology, supported by the posterior accumulation of KHC1-910GFP (supplementary material Fig. S6J-N; Fig. 5B). Thus, it could be that the AMB site is affecting *oskar* RNP binding specifically and not via any MT-related activity. This hypothesis is supported by the fact that there are several proteins that interact with the KHC tail, including Kv3.1 (Shaw – FlyBase), which binds the region containing the AMB domain and requires it for its transport (Xu et al., 2010).

The localization of *oskar* RNA in KHC1-938 and KHC1-975ΔIAK oocytes is not completely wild type, since ‘dots/clouds’ of the transcript are observed in close proximity to the posterior. Dots/clouds of *oskar* at the posterior is a phenotype observed in oocytes with minor MT defects, *oskar* translation defects (Zimyanin et al., 2007), slower KHC (Loiseau et al., 2010; Serbus et al., 2005; Moua et al., 2011) or upregulated KHC (Krauss et al., 2009). We do not know why there is an *oskar* ‘dot’ phenotype in KHC1-938 and KHC1-975ΔIAK oocytes. There are no obvious MT defects at the posterior of these mutants (supplementary material Fig. S6J-N), although the mutant motors are found in the *oskar* dots, which might suggest the presence of plus ends. This dots phenotype is also seen in *Rab6* and *Rab11* mutants (Coutelis and Ephrussi, 2007; Dollar et al., 2002; Jankovics et al., 2001; Januschke et al., 2007) and it might thus be related to a vesicle trafficking function of KHC. This idea is supported by our findings, since KHC1-975ΔIAK and KHC1-938 oocytes show aberrant actin spheres/vesicles (84% and 45% of KHC1-975ΔIAK and KHC1-938 oocytes, respectively) and dots/clouds of *oskar* adjacent to the posterior crescent. The relationship between *oskar* localization, MTs and endocytosis at the posterior is complex, involving various feedback loops (Tanaka et al., 2011; Tanaka and Nakamura, 2008; Vanzo et al., 2007). It is possible that defects in vesicle trafficking result in mild defects in cytoskeleton organization, since *Rab11* and *Rab6* mutant oocytes show mispolarized MTs. Thus, this inefficient *oskar* localization to a posterior crescent in mutant oocytes might indirectly result from mild cytoskeleton defects at the posterior. Alternatively, KHC1-975ΔIAK-dependent or KHC1-938-dependent ectopic *Oskar* protein and/or ectopic MT plus ends might result in aberrant endocytosis at the posterior.

It is interesting to note that although *oskar* RNA is not a conserved cargo its transport involves a highly conserved domain, i.e. the AMB domain. This, and our findings concerning the IAK domain, show that although not all cargoes are conserved their transport involves the most conserved domains of animal KHCs. Thus, both the IAK and AMB domains might play a crucial role in the transport of cargoes in other cell types and organisms.

MATERIALS AND METHODS

Stocks and germline clones

Fly stocks: *yw*[−], *P{ry⁺};hs:FLP*; *P{w⁺,FRT}G13* *ovoD¹/Tp/CyO*, *w[−],P{w⁺,FRT}G13Khc²⁷/CyO*; *P{w⁺, mat-tub-α4:KHC1-975GFP}/TM6B*,

$w^{-}, P\{w^{+}, FRT\}G13Khc^{27}/CyO; P\{w^{+}, mat-tub-\alpha4:KHC1-975\Delta IAKGFP\}/TM6B, w^{-}, P\{w^{+}, FRT\}G13Khc^{27}/CyO; P\{w^{+}, mat-tub-\alpha4:KHC1-950GFP\}/TM6B, w^{-}, P\{w^{+}, mat-tub-\alpha4:KHC1-849GFP\}/FM7; P\{w^{+}, FRT\}G13Khc^{27}/CyO, w^{-}, P\{w^{+}, mat-tub-\alpha4:KHC1-910GFP\}/FM7; P\{w^{+}, FRT\}G13Khc^{27}/CyO, w^{-}, P\{w^{+}, FRT\}G13Khc^{27}/CyO; P\{w^{+}, mat-tub-\alpha4:KHC1-700GFP\}/TM6B, w^{-}, P\{w^{+}, FRT\}G13Khc^{27}/CyO; P\{w^{+}, mat-tub-\alpha4:KHC231-975GFP\}/TM6B, yw^{-}, Kin1-604betaGal/FM7i; P\{w^{+}, FRT\}G13Khc^{27}/CyO, w^{-}, P\{w^{+}, mat-tub-\alpha4:KHC330-975GFP\}/FM7; P\{w^{+}, FRT\}G13Khc^{27}/CyO, yw^{-}, P\{ry^{+}; hs:FLP\}; P\{w^{+}, FRT\}G13GFP; P\{w^{+}, mat-tub-\alpha4:KHC231-975GFP, w^{-}, P\{w^{+}, FRT\}G13Khc^{27}/CyO, w^{-}, P\{w^{+}, FRT\}G13Khc^{23}/CyO, w^{-}, P\{w^{+}, FRT\}G13Khc^{17}/CyO. Germline clones for *Khc* were created by the FLP/FRT system (Chou et al., 1993; Chou and Perrimon, 1996). Homozygous clones generated by heat-shocking L3 for 2 hours at 37°C for 3 days were selected by the *ovoD* system or by the absence of GFP.$

Transgenic constructs

Mutagenesis was performed using the QuikChange II XL Lightning Site-Directed Mutagenesis Kit (Stratagene). The KHC region to be cloned was ligated into pD277-GFP6 (van Eeden et al., 2001) to create a construct in which KHC, fused to GFP at its C-terminus, was expressed under the control of the maternal tubulin promoter.

Immunohistochemistry and western blotting

Immunostaining with Staufin [1:3000 (St Johnston et al., 1991)], Dynein (1:250, DSHB, 2C11-2-s) and Gurken (1:10, DSHB, 1D12) antibodies were performed as described (Palacios and St Johnston, 2002). For immunostaining with rat alpha-tubulin antibody (1:100, Millipore, MAB1864), ovaries were fixed in 4% paraformaldehyde (PFA) for 20 minutes, incubated with BRB80 (80 mM PIPES pH 6.8, 1 mM MgCl₂, 1 mM EGTA) containing 1% Triton X-100 for 1 hour at 25°C without agitation, fixed with methanol at -20°C for 15 minutes, rehydrated for 15 hours at 4°C with 2% Tween 20 in PBS, and then blocked in 2% Tween 20 and 2% BSA in PBS for 1 hour at room temperature. After incubation with the alpha-tubulin antibody overnight (2% Tween 20, 2% BSA in PBS), the ovaries were washed twice for 15 minutes each with 0.2% Tween 20 in PBS and then incubated with the secondary antibody (Invitrogen Alexa 568 nm A11077) in 2% Tween 20 and 1% BSA in PBS. After washing twice for 15 minutes each in 0.2% Tween 20 in PBS, the ovaries were mounted in Vectashield with DAPI (Vector Laboratories) (Januschke et al., 2006). For mouse FITC-alpha-tubulin (1:250, Sigma), the protocol was as described above except that rehydration and blocking were performed with 0.2% Tween 20 in PBS and no secondary antibody was used.

For western blots, four ovaries were dissected in 1× protein loading buffer in PBS, homogenized and run on 10% SDS-PAGE gels. Antibodies were mouse anti-GFP (1:2500, Invitrogen, 3E6, A11120) and anti-KHC (1:1000, Cytoskeleton, AKIN01).

Live imaging

Cytoplasmic streaming was observed in live st9 and st11 oocytes. Females were fattened on yeast for 20 hours at 25°C. Ovaries were dissected in 10S Voltalef oil (Altachem) and examined under a 40×/1.3 oil DIC Plan-Neofluar objective (Zeiss) using a Leica LSM inverted confocal microscope. For st9 or st11 oocytes, autofluorescent particles were imaged that reflected the 561 nm or 405 nm laser lines, respectively. Movies were 100–500 frames long at a scan speed of 200 Hz. Flow architectures were defined using the correlation length, a statistical quantity giving the radii of the flow features observed (Ganguly et al., 2012).

Acknowledgements

We thank Prof. Davis and Prof. Gavis for comments; M. Wayland for assistance with imaging; Drs Nakamura, St Johnston and Saxton for reagents; and especially Dr Geldfand for the KHCΔHinge2 DNA.

Competing interests

The authors declare no competing financial interests.

Author contributions

L.S.W. designed and performed experiments and analyzed the data. L.S.W. and I.M.P. designed experiments, discussed results and wrote the manuscript. B.F.N. performed and analyzed some experiments. S.G. analyzed flows by particle image

velocimetry and discussed results. P.L. designed some of the transgenic constructs and performed and discussed early experiments.

Funding

L.S.W. and P.L. were supported by the Wellcome Trust and L.S.W. by the Cambridge Cancer Centre/Cancer Research UK; S.G. by the European Research Council; B.F.N. by Singapore Ministry of Education; and I.M.P. by the Royal Society and Cambridge University. Deposited in PMC for immediate release.

Supplementary material

Supplementary material available online at <http://dev.biologists.org/lookup/suppl/doi:10.1242/dev.097592/-DC1>

References

- Abdu, U., Bar, D. and Schüpbach, T. (2006). *spn-F* encodes a novel protein that affects oocyte patterning and bristle morphology in *Drosophila*. *Development* **133**, 1477–1484.
- Al-Bassam, J., Cui, Y., Klopstein, D., Carragher, B. O., Vale, R. D. and Milligan, R. A. (2003). Distinct conformations of the kinesin Unc104 neck regulate a monomer to dimer motor transition. *J. Cell Biol.* **163**, 743–753.
- Arimoto, M., Koushika, S. P., Choudhary, B. C., Li, C., Matsumoto, K. and Hisamoto, N. (2011). The *Caenorhabditis elegans* JIP3 protein UNC-16 functions as an adaptor to link kinesin-1 with cytoplasmic dynein. *J. Neurosci.* **31**, 2216–2224.
- Barlan, K., Lu, W. and Gelfand, V. I. (2013). The microtubule-binding protein enscosin is an essential cofactor of kinesin-1. *Curr. Biol.* **23**, 317–322.
- Bowman, A. B., Kamal, A., Ritchings, B. W., Philp, A. V., McGrail, M., Gindhart, J. G. and Goldstein, L. S. (2000). Kinesin-dependent axonal transport is mediated by the sunday driver (SYD) protein. *Cell* **103**, 583–594.
- Brendza, R. P., Serbus, L. R., Duffy, J. B. and Saxton, W. M. (2000). A function for kinesin I in the posterior transport of *oskar* mRNA and Staufin protein. *Science* **289**, 2120–2122.
- Brendza, R. P., Serbus, L. R., Saxton, W. M. and Duffy, J. B. (2002). Posterior localization of dynein and dorsal-ventral axis formation depend on kinesin in *Drosophila* oocytes. *Curr. Biol.* **12**, 1541–1545.
- Cha, B. J., Serbus, L. R., Koppetsch, B. S. and Theurkauf, W. E. (2002). Kinesin I-dependent cortical exclusion restricts pole plasm to the oocyte posterior. *Nat. Cell Biol.* **4**, 592–598.
- Chou, T. B. and Perrimon, N. (1996). The autosomal FLP-DFS technique for generating germline mosaics in *Drosophila melanogaster*. *Genetics* **144**, 1673–1679.
- Chou, T.-B., Noll, E. and Perrimon, N. (1993). Autosomal P[ovo^{D1}] dominant female-sterile insertions in *Drosophila* and their use in generating germ-line chimeras. *Development* **119**, 1359–1369.
- Compagnon, J., Gervais, L., Roman, M. S., Chamot-Boeuf, S. and Guichet, A. (2009). Interplay between Rab5 and PtdIns(4,5)P₂ controls early endocytosis in the *Drosophila* germline. *J. Cell Sci.* **122**, 25–35.
- Coutelis, J. B. and Ephrussi, A. (2007). Rab6 mediates membrane organization and determinant localization during *Drosophila* oogenesis. *Development* **134**, 1419–1430.
- Coy, D. L., Hancock, W. O., Wagenbach, M. and Howard, J. (1999). Kinesin's tail domain is an inhibitory regulator of the motor domain. *Nat. Cell Biol.* **1**, 288–92.
- Dahlgard, K., Raposo, A. A., Niccoli, T. and St Johnston, D. (2007). Capu and Spire assemble a cytoplasmic actin mesh that maintains microtubule organization in the *Drosophila* oocyte. *Dev. Cell* **13**, 539–553.
- Delanoue, R. and Davis, I. (2005). Dynein anchors its mRNA cargo after apical transport in the *Drosophila* blastoderm embryo. *Cell* **122**, 97–106.
- Delanoue, R., Herpers, B., Soetaert, J., Davis, I. and Rabouille, C. (2007). *Drosophila* Squid/hnRNP helps Dynein switch from a gurken mRNA transport motor to an ultrastructural static anchor in sponge bodies. *Dev. Cell* **13**, 523–538.
- Diefenbach, R. J., Mackay, J. P., Armati, P. J. and Cunningham, A. L. (1998). The C-terminal region of the stalk domain of ubiquitous human kinesin heavy chain contains the binding site for kinesin light chain. *Biochemistry* **37**, 16663–16670.
- Dollar, G., Struckhoff, E., Michaud, J. and Cohen, R. S. (2002). Rab11 polarization of the *Drosophila* oocyte: a novel link between membrane trafficking, microtubule organization, and *oskar* mRNA localization and translation. *Development* **129**, 517–526.
- Duncan, J. E. and Warrior, R. (2002). The cytoplasmic dynein and kinesin motors have interdependent roles in patterning the *Drosophila* oocyte. *Curr. Biol.* **12**, 1982–1991.
- Forrest, K. M. and Gavis, E. R. (2003). Live imaging of endogenous RNA reveals a diffusion and entrapment mechanism for nanos mRNA localization in *Drosophila*. *Curr. Biol.* **13**, 1159–1168.
- Friedman, D. S. and Vale, R. D. (1999). Single-molecule analysis of kinesin motility reveals regulation by the cargo-binding tail domain. *Nat. Cell Biol.* **1**, 293–297.
- Gagnon, J. A. and Mowry, K. L. (2011). Molecular motors: directing traffic during RNA localization. *Crit. Rev. Biochem. Mol. Biol.* **46**, 229–239.
- Ganguly, S., Williams, L. S., Palacios, I. M. and Goldstein, R. E. (2012). Cytoplasmic streaming in *Drosophila* oocytes varies with kinesin activity and correlates with the microtubule cytoskeleton architecture. *Proc. Natl. Acad. Sci. USA* **109**, 15109–15114.
- Gauger, A. K. and Goldstein, L. S. (1993). The *Drosophila* kinesin light chain. Primary structure and interaction with kinesin heavy chain. *J. Biol. Chem.* **268**, 13657–13666.
- Genniferich, A. and Vale, R. D. (2009). Walking the walk: how kinesin and dynein coordinate their steps. *Curr. Opin. Cell Biol.* **21**, 59–67.

- Gervais, L., Claret, S., Januschke, J., Roth, S. and Guichet, A. (2008). PIP5K-dependent production of PIP2 sustains microtubule organization to establish polarized transport in the *Drosophila* oocyte. *Development* **135**, 3829-3838.
- Gindhart, J. G., Jr, Desai, C. J., Beushausen, S., Zinn, K. and Goldstein, L. S. (1998). Kinesin light chains are essential for axonal transport in *Drosophila*. *J. Cell Biol.* **141**, 443-454.
- Glater, E. E., Megeath, L. J., Stowers, R. S. and Schwarz, T. L. (2006). Axonal transport of mitochondria requires mltin to recruit kinesin heavy chain and is light chain independent. *J. Cell Biol.* **173**, 545-557.
- Hackney, D. D. and Stock, M. F. (2000). Kinesin's IAK tail domain inhibits initial microtubule-stimulated ADP release. *Nat. Cell Biol.* **2**, 257-260.
- Hackney, D. D., Baek, N. and Snyder, A. C. (2009). Half-site inhibition of dimeric kinesin head domains by monomeric tail domains. *Biochemistry* **48**, 3448-3456.
- Hirokawa, N., Niwa, S. and Tanaka, Y. (2010). Molecular motors in neurons: transport mechanisms and roles in brain function, development, and disease. *Neuron* **68**, 610-638.
- Imanishi, M., Endres, N. F., Gennerich, A. and Vale, R. D. (2006). Autoinhibition regulates the motility of the *C. elegans* intraflagellar transport motor OSM-3. *J. Cell Biol.* **174**, 931-937.
- Jankovics, F., Sinka, R. and Erdélyi, M. (2001). An interaction type of genetic screen reveals a role of the Rab11 gene in oskar mRNA localization in the developing *Drosophila melanogaster* oocyte. *Genetics* **158**, 1177-1188.
- Januschke, J., Gervais, L., Dass, S., Kaltschmidt, J. A., Lopez-Schier, H., St Johnston, D., Brand, A. H., Roth, S. and Guichet, A. (2002). Polar transport in the *Drosophila* oocyte requires Dynein and Kinesin I cooperation. *Curr. Biol.* **12**, 1971-1981.
- Januschke, J., Gervais, L., Gillet, L., Keryer, G., Bornens, M. and Guichet, A. (2006). The centrosome-nucleus complex and microtubule organization in the *Drosophila* oocyte. *Development* **133**, 129-139.
- Januschke, J., Nicolas, E., Compagnon, J., Formstecher, E., Goud, B. and Guichet, A. (2007). Rab6 and the secretory pathway affect oocyte polarity in *Drosophila*. *Development* **134**, 3419-3425.
- Jolly, A. L., Kim, H., Srinivasan, D., Lakonishok, M., Larson, A. G. and Gelfand, V. I. (2010). Kinesin-1 heavy chain mediates microtubule sliding to drive changes in cell shape. *Proc. Natl. Acad. Sci. USA* **107**, 12151-12156.
- Jung, H. S., Komatsu, S., Ikebe, M. and Craig, R. (2008). Head-head and head-tail interaction: a general mechanism for switching off myosin II activity in cells. *Mol. Biol. Cell* **19**, 3234-3242.
- Karle, K. N., Möckel, D., Reid, E. and Schöls, L. (2012). Axonal transport deficit in a KIF5A(-/-) mouse model. *Neurogenetics* **13**, 169-179.
- Karpova, N., Bobiniec, Y., Fouix, S., Huitorel, P. and Debec, A. (2006). Jupiter, a new *Drosophila* protein associated with microtubules. *Cell Motil. Cytoskeleton* **63**, 301-312.
- Kirchner, J., Seiler, S., Fuchs, S. and Schliwa, M. (1999a). Functional anatomy of the kinesin molecule in vivo. *EMBO J.* **18**, 4404-4413.
- Kirchner, J., Woehlke, G. and Schliwa, M. (1999b). Universal and unique features of kinesin motors: insights from a comparison of fungal and animal conventional kinesins. *Biol. Chem.* **380**, 915-921.
- Kugler, J. M., Chicoine, J. and Lasko, P. (2009). Bicaudal-C associates with a Trailer Hitch/Me31B complex and is required for efficient Gurken secretion. *Dev. Biol.* **328**, 160-172.
- Lei, Y. and Warrior, R. (2000). The *Drosophila* Lissencephaly1 (DLis1) gene is required for nuclear migration. *Dev. Biol.* **226**, 57-72.
- Li, X. D., Jung, H. S., Mabuchi, K., Craig, R. and Ikebe, M. (2006). The globular tail domain of myosin Va functions as an inhibitor of the myosin Va motor. *J. Biol. Chem.* **281**, 21789-21798.
- Ligon, L. A., Tokito, M., Finklestein, J. M., Grossman, F. E. and Holzbaur, E. L. (2004). A direct interaction between cytoplasmic dynein and kinesin I may coordinate motor activity. *J. Biol. Chem.* **279**, 19201-19208.
- Ling, S. C., Fahrner, P. S., Greenough, W. T. and Gelfand, V. I. (2004). Transport of *Drosophila* fragile X mental retardation protein-containing ribonucleoprotein granules by kinesin-1 and cytoplasmic dynein. *Proc. Natl. Acad. Sci. USA* **101**, 17428-17433.
- Loiseau, P., Davies, T., Williams, L. S., Mishima, M. and Palacios, I. M. (2010). *Drosophila* PAT1 is required for Kinesin-1 to transport cargo and to maximize its motility. *Development* **137**, 2763-2772.
- Meyerzon, M., Fridolfsson, H. N., Ly, N., McNally, F. J. and Starr, D. A. (2009). UNC-83 is a nuclear-specific cargo adaptor for kinesin-1-mediated nuclear migration. *Development* **136**, 2725-2733.
- Mische, S., Li, M., Serr, M. and Hays, T. S. (2007). Direct observation of regulated ribonucleoprotein transport across the nurse cell/oocyte boundary. *Mol. Biol. Cell* **18**, 2254-2263.
- Moua, P., Fullerton, D., Serbus, L. R., Warrior, R. and Saxton, W. M. (2011). Kinesin-1 tail autoregulation and microtubule-binding regions function in saltatory transport but not ooplasmic streaming. *Development* **138**, 1087-1092.
- Navone, F., Niclas, J., Hom-Booher, N., Sparks, L., Bernstein, H. D., McCaffrey, G. and Vale, R. D. (1992). Cloning and expression of a human kinesin heavy chain gene: interaction of the COOH-terminal domain with cytoplasmic microtubules in transfected CV-1 cells. *J. Cell Biol.* **117**, 1263-1275.
- Neuman-Silberberg, F. S. and Schüpbach, T. (1993). The *Drosophila* dorsoventral patterning gene gurken produces a dorsally localized RNA and encodes a TGF alpha-like protein. *Cell* **75**, 165-174.
- Palacios, I. M. and St Johnston, D. (2002). Kinesin light chain-independent function of the Kinesin heavy chain in cytoplasmic streaming and posterior localisation in the *Drosophila* oocyte. *Development* **129**, 5473-5485.
- Parton, R. M., Hamilton, R. S., Ball, G., Yang, L., Cullen, C. F., Lu, W., Ohkura, H. and Davis, I. (2011). A PAR-1-dependent orientation gradient of dynamic microtubules directs posterior cargo transport in the *Drosophila* oocyte. *J. Cell Biol.* **194**, 121-135.
- Rauzi, M., Lenne, P. F. and Lecuit, T. (2010). Planar polarized actomyosin contractile flows control epithelial junction remodelling. *Nature* **468**, 1110-1114.
- Seeger, M. A. and Rice, S. E. (2010). Microtubule-associated protein-like binding of the kinesin-1 tail to microtubules. *J. Biol. Chem.* **285**, 8155-8162.
- Seiler, S., Kirchner, J., Horn, C., Kallipolitou, A., Woehlke, G. and Schliwa, M. (2000). Cargo binding and regulatory sites in the tail of fungal conventional kinesin. *Nat. Cell Biol.* **2**, 333-338.
- Serbus, L. R., Cha, B. J., Theurkauf, W. E. and Saxton, W. M. (2005). Dynein and the actin cytoskeleton control kinesin-driven cytoplasmic streaming in *Drosophila* oocytes. *Development* **132**, 3743-3752.
- Setou, M., Seog, D. H., Tanaka, Y., Kanai, Y., Takei, Y., Kawagishi, M. and Hirokawa, N. (2002). Glutamate-receptor-interacting protein GRIP1 directly steers kinesin to dendrites. *Nature* **417**, 83-87.
- Shapiro, R. S. and Anderson, K. V. (2006). *Drosophila* Ik2, a member of the I kappa B kinase family, is required for mRNA localization during oogenesis. *Development* **133**, 1467-1475.
- Shubeita, G. T., Tran, S. L., Xu, J., Vershinin, M., Cermelli, S., Cotton, S. L., Welte, M. A. and Gross, S. P. (2008). Consequences of motor copy number on the intracellular transport of kinesin-1-driven lipid droplets. *Cell* **135**, 1098-1107.
- Skoufias, D. A., Cole, D. G., Wedaman, K. P. and Scholey, J. M. (1994). The carboxyl-terminal domain of kinesin heavy chain is important for membrane binding. *J. Biol. Chem.* **269**, 1477-1485.
- Snee, M. J. and Macdonald, P. M. (2009). Bicaudal C and trailer hitch have similar roles in gurken mRNA localization and cytoskeletal organization. *Dev. Biol.* **328**, 434-444.
- Splinter, D., Tanenbaum, M. E., Lindqvist, A., Jaarsma, D., Flotho, A., Yu, K. L., Grigoriev, I., Engelsma, D., Haasdijk, E. D., Keijzer, N. et al. (2010). Bicaudal D2, dynein, and kinesin-1 associate with nuclear pore complexes and regulate centrosome and nuclear positioning during mitotic entry. *PLoS Biol.* **8**, e1000350.
- St Johnston, D., Beuchle, D. and Nüsslein-Volhard, C. (1991). Stauf, a gene required to localize maternal RNAs in the *Drosophila* egg. *Cell* **66**, 51-63.
- Stock, M. F., Guerrero, J., Cobb, B., Eggers, C. T., Huang, T. G., Li, X. and Hackney, D. D. (1999). Formation of the compact conformation of kinesin requires a COOH-terminal heavy chain domain and inhibits microtubule-stimulated ATPase activity. *J. Biol. Chem.* **274**, 14617-14623.
- Straube, A., Hause, G., Fink, G. and Steinberg, G. (2006). Conventional kinesin mediates microtubule-microtubule interactions in vivo. *Mol. Biol. Cell* **17**, 907-916.
- Sun, F., Zhu, C., Dixit, R. and Cavalli, V. (2011). Sunday Driver/JIP3 binds kinesin heavy chain directly and enhances its motility. *EMBO J.* **30**, 3416-3429.
- Swan, A. and Suter, B. (1996). Role of Bicaudal-D in patterning the *Drosophila* egg chamber in mid-oogenesis. *Development* **122**, 3577-3586.
- Swan, A., Nguyen, T. and Suter, B. (1999). *Drosophila* Lissencephaly-1 functions with Bic-D and dynein in oocyte determination and nuclear positioning. *Nat. Cell Biol.* **1**, 444-449.
- Tanaka, T. and Nakamura, A. (2008). The endocytic pathway acts downstream of Oskar in *Drosophila* germ plasm assembly. *Development* **135**, 1107-1117.
- Tanaka, T., Kato, Y., Matsuda, K., Hanyu-Nakamura, K. and Nakamura, A. (2011). *Drosophila* Mon2 couples Oskar-induced endocytosis with actin remodeling for cortical anchorage of the germ plasm. *Development* **138**, 2523-2532.
- Taya, S., Shinoda, T., Tsuboi, D., Asaki, J., Nagai, K., Hikita, T., Kuroda, S., Kuroda, K., Shimizu, M., Hirotsune, S. et al. (2007). DISC1 regulates the transport of the NUDEL/LIS1/14-3-3epsilon complex through kinesin-1. *J. Neurosci.* **27**, 15-26.
- Technau, M. and Roth, S. (2008). The *Drosophila* KASH domain proteins Msp-300 and Klarsicht and the SUN domain protein Klaroid have no essential function during oogenesis. *Fly (Austin)* **2**, 82-91.
- Theurkauf, W. E. (1994). Premature microtubule-dependent cytoplasmic streaming in cappuccino and spire mutant oocytes. *Science* **265**, 2093-2096.
- Umeki, N., Jung, H. S., Watanabe, S., Sakai, T., Li, X. D., Ikebe, R., Craig, R. and Ikebe, M. (2009). The tail binds to the head-neck domain, inhibiting ATPase activity of myosin VIIA. *Proc. Natl. Acad. Sci. USA* **106**, 8483-8488.
- van Eeden, F. J., Palacios, I. M., Petronczki, M., Weston, M. J. and St Johnston, D. (2001). Barentsz is essential for the posterior localization of oskar mRNA and colocalizes with it to the posterior pole. *J. Cell Biol.* **154**, 511-524.
- Vanzo, N., Oprins, A., Xanthakis, D., Ephrussi, A. and Rabouille, C. (2007). Stimulation of endocytosis and actin dynamics by Oskar polarizes the *Drosophila* oocyte. *Dev. Cell* **12**, 543-555.
- Verhey, K. J., Meyer, D., Deehan, R., Blenis, J., Schnapp, B. J., Rapoport, T. A. and Margolis, B. (2001). Cargo of kinesin identified as JIP scaffolding proteins and associated signaling molecules. *J. Cell Biol.* **152**, 959-970.
- Welte, M. A. (2009). Fat on the move: intracellular motion of lipid droplets. *Biochem. Soc. Trans.* **37**, 991-996.
- Xu, M., Gu, Y., Barry, J. and Gu, C. (2010). Kinesin I transports tetramerized Kv3 channels through the axon initial segment via direct binding. *J. Neurosci.* **30**, 15987-16001.
- Yonekura, H., Nomura, A., Ozawa, H., Tatsu, Y., Yumoto, N. and Uyeda, T. Q. (2006). Mechanism of tail-mediated inhibition of kinesin activities studied using synthetic peptides. *Biochem. Biophys. Res. Commun.* **343**, 420-427.
- Yu, H., Toyoshima, I., Steuer, E. R. and Sheetz, M. P. (1992). Kinesin and cytoplasmic dynein binding to brain microtubules. *J. Biol. Chem.* **267**, 20457-20464.
- Zhao, T., Graham, O. S., Raposo, A. and St Johnston, D. (2012). Growing microtubules push the oocyte nucleus to polarize the *Drosophila* dorsal-ventral axis. *Science* **336**, 999-1003.
- Zimyanin, V., Lowe, N. and St Johnston, D. (2007). An oskar-dependent positive feedback loop maintains the polarity of the *Drosophila* oocyte. *Curr. Biol.* **17**, 353-359.